



# **Tunable Single-frequency operation of a diode-pumped Vertical-External Cavity Laser at the Caesium D2 line**

Benjamin Cocquelin, David Holleville, Gaëlle Lucas-Leclin, Isabelle Sagnes, Arnaud Garnache, Mikhaël Myara, Patrick Georges

## **► To cite this version:**

Benjamin Cocquelin, David Holleville, Gaëlle Lucas-Leclin, Isabelle Sagnes, Arnaud Garnache, et al.. Tunable Single-frequency operation of a diode-pumped Vertical-External Cavity Laser at the Caesium D2 line. *Applied Physics B - Laser and Optics*, 2009, 95 (2), pp.315-321. 10.1007/s00340-008-3361-3 . hal-00523979

**HAL Id: hal-00523979**

**<https://hal-iogs.archives-ouvertes.fr/hal-00523979>**

Submitted on 6 Oct 2010

**HAL** is a multi-disciplinary open access archive for the deposit and dissemination of scientific research documents, whether they are published or not. The documents may come from teaching and research institutions in France or abroad, or from public or private research centers.

L'archive ouverte pluridisciplinaire **HAL**, est destinée au dépôt et à la diffusion de documents scientifiques de niveau recherche, publiés ou non, émanant des établissements d'enseignement et de recherche français ou étrangers, des laboratoires publics ou privés.

# Tunable Single-frequency operation of a diode-pumped Vertical-External Cavity Laser at the Caesium D<sub>2</sub> line

B. Cocquelin<sup>1</sup>, D. Holleville<sup>2</sup>, G. Lucas-Leclin<sup>1\*</sup>, I. Sagnes<sup>3</sup>, A. Garnache<sup>4</sup>, M. Myara<sup>4</sup>, P. Georges<sup>1</sup>

1. Laboratoire Charles Fabry de l'Institut d'Optique, CNRS, Univ Paris Sud, Campus Polytechnique, RD 128  
91127 Palaiseau, France

2. LNE-SYRTE, Systèmes de Référence Temps-Espace, UMR 8630 CNRS, , Observatoire de Paris,  
61 avenue de l'Observatoire 75014 Paris, France

3. Laboratoire de Photonique et de Nanostructures CNRS UPR20, Route de Nozay, 91460 Marcoussis, France

4. Institut d'Electronique du Sud, CNRS UMR 5214, Université Montpellier II, 34095 Montpellier, France

\* Corresponding author : fax: +33 1 64 53 31 01, e-mail: gaelle.lucas-leclin@institutoptique.fr

**Abstract:** We report on a diode-pumped vertical external-cavity surface-emitting laser emitting around 852 nm for Cesium atomic clocks experiments. We have designed a 7-quantum-well semiconductor structure optimized for low laser threshold. An output power of 330 mW was achieved for 1.1 W of incident pump power. Furthermore a compact setup was built for low-power single-frequency emission. We obtained an output power of 17 mW in a single longitudinal mode, exhibiting both broad (9 nm) and continuous (14 GHz) tunability around the Cesium D<sub>2</sub> line. The laser frequency has been stabilized on an atomic transition with residual frequency fluctuations  $\sim 300$  kHz. Through a beatnote experiment the -3 dB laser linewidth has been measured to  $< 500$  kHz over 10 ms.

**PACS:** 42.55.Px Semiconductor lasers; laser diodes; 42.62.Eh Metrological applications; 42.55.Xi Diode-pumped lasers

## 1. Introduction

Cold-atom interferometry experiments require demanding efforts for laser sources in terms of spectral and power performances. One of the most popular atomic species is <sup>133</sup>Cs, which gives the reference for the definition of the second since 1967, and is used in atomic frequency standards [1,2] as well as in atomic inertial sensors [3]. For these applications, complex laser benches are used to perform trapping, cooling, manipulation and optical detection of atoms [2,4]. Actually the different stages of these cold-atom experiments have distinct constraints on laser sources, such as high output power ( $> 200$  mW) for efficient atom cooling or stimulated-Raman transitions, but narrow-linewidth emission ( $< 500$  kHz) for optical detection. In any case, stable single-frequency operation and fine tunability over a few GHz around the atomic transitions are requested. Currently, available laser sources show intrinsic limitations in fulfilling all the required properties : Extended-Cavity Diode Lasers (ECDL) do not deliver more than  $\sim 50$  mW but have usually linewidths below 200 kHz [5,6]; Master Oscillator-Power Amplifier (MOPA) systems, which consists in a semiconductor amplifier optically injected by an ECDL, may increase the available power with a moderate broadening of the laser spectral line, but require complicated mechanical engineering as well as thermal management and complex beam shaping [7,8]; Distributed Feedback laser diodes (DFB) [9] have actually demonstrated single-frequency operation up to 0.25 W with sub-MHz linewidths, and Tapered Extended-Cavity Lasers [6,10] are high-power evolution of standard ECDL, with narrow linewidth ( $< 10$  MHz) and output power in the Watt range. These two latter solutions, both based on wavelength-stabilized laser diodes, are promising but suffer from degradation of the beam quality and of the linewidth at high power. Consequently in cold-atom experiments, several lasers are used simultaneously to provide different optical features, while a single laser source would greatly improve the compactness, the efficiency and the simplicity of these set-ups

Optically-pumped Vertical External-Cavity Surface-Emitting Lasers (VECSELs) combine the approach of diode-pumped solid-state lasers and engineered semiconductor lasers, generating both circular diffraction limited output beams and high powers [11,12]. These lasers benefit from the knowledge in semiconductor fabrication to grow high reflectivity multilayer Bragg mirrors and good quality multiple-quantum-well gain structures operating in external cavities. The power scaling possibilities of these semiconductor thin disks to obtain multi-watts output powers have already been demonstrated [13]. Furthermore the utilization of a resonant periodic gain (RPG) design ensures a spatially- and spectrally-homogeneous gain, which is favourable for single-frequency operation [14]. Actually this has already been obtained in simple and compact laser cavities [15,16], and laser linewidths in the range of few kHz have been measured by comparison with Fabry-Perot reference cavities [16-18]. VECSELs appear then to be an interesting way to achieve compact and efficient single-frequency sources for demanding applications such as metrology and spectroscopy.

In this paper we present the design of a specific structure emitting near 852 nm - corresponding to the Cs D<sub>2</sub> line. The number of quantum wells has been optimized in order to get a low threshold pump power and still a

relatively high optical gain. We have made a diode-pumped VECSEL emitting 330 mW in a transverse single-mode operation with a semiconductor active device on a GaAs substrate. Finally, in a very simple and compact cavity setup, we studied the coarse and fine tunability of the single frequency emission around the Cesium D<sub>2</sub> line. The frequency stabilization on an atomic line has been performed, and the laser linewidth has been characterized through a beat note with a reference laser.

## 2. Description of the semiconductor structure

The active region of the semiconductor structure has been specifically designed for laser emission around 852 nm. It is optically pumped in the quantum-well barriers, which prescribes a pump wavelength below 720 nm. Since red laser sources are neither as efficient nor as powerful in that spectral range than in the infrared, the active structure need to be carefully designed with the aim to reach a low laser threshold while keeping the highest gain achievable. We have especially optimized the number of quantum wells (QWs) and their position in the active region. The pump intensity at threshold  $I_{th}$  is expressed as a function of the roundtrip losses  $L$  :

$$I_{th} = N_{QW} I_{tr} \times \exp\left(\frac{L}{2N_{QW} L_{QW} \Gamma g_0}\right) \quad (1)$$

where  $L_{QW}$  and  $N_{QW}$  are respectively the thickness and the number of QWs,  $\Gamma = 2$  is the longitudinal confinement factor and  $I_{inc}$  the incident pump intensity [19]. From the experimental characterization of  $I_{th}$  as a function of intracavity losses at different device temperature  $T$  [20], a linear gain per well  $g_0 = 1000 \text{ cm}^{-1}$  and an incident pump intensity at transparency per quantum well  $I_{tr} = 105 \text{ W/cm}^2$  have been considered at  $T = 10^\circ\text{C}$ , and  $g_0 = 830 \text{ cm}^{-1}$  and  $I_{tr} = 105 \text{ W/cm}^2$  at  $T = 40^\circ\text{C}$ . According to Figure 1, seven QWs correspond to an optimum which minimizes the pump intensity at threshold for roundtrip losses (including output coupler transmission) about a few percents, even at high temperature. Further increase of the QWs number would result in a larger threshold intensity.

The semiconductor chip (so-called  $\frac{1}{2}$ -VCSEL) has been grown by metal-organic chemical-vapor deposition on a 350- $\mu\text{m}$  thick GaAs substrate. It contains a multilayer Distributed Bragg Reflector (DBR) and an active region (Figure 2). The DBR bottom mirror consists of 32.5 pairs of  $\text{AlAs}/\text{Al}_{0.225}\text{Ga}_{0.775}\text{As}$  quarter-wave layers resulting in a 99.95 %-reflectivity 70-nm-wide stop-band centered on 852 nm. Grown on the top of the Bragg mirror is the  $29 \lambda/4$ -thick anti-resonant cavity; seven 8-nm thick GaAs QWs, embedded between  $\text{Al}_{0.225}\text{Ga}_{0.775}\text{As}$  barriers, are distributed among the optical standing-wave antinodes positions, with a repartition 1-1-1-1-0-1-0-1-0-1 (from the top surface) which has been calculated in order that the excited carrier density remains constant in all QWs and about 14% of the total photogenerated electron-hole pairs. The pump absorption in the barriers is evaluated to 90% in single-pass for wavelengths around 680 nm. Finally, two 30 nm-thick  $\text{Al}_{0.39}\text{Ga}_{0.61}\text{As}$  layers produces a potential barrier at the Bragg mirror/active region interface and at the top surface for carrier confinement, and the structure has been protected by a 20 nm-thick  $\text{In}_{0.48}\text{Ga}_{0.52}\text{P}$  capping layer against oxidation of the Al-rich barrier layers. This cap layer is requisite to improve the operating lifetime of the structure; no degradation nor failure have been observed within months of laser operation under high power pumping. In the end the wafer is anti-reflection coated at 852 nm with a  $\lambda/4$   $\text{Si}_3\text{N}_4$  layer to increase the transmission of the incident pump laser and to reduce any intracavity etalon effect at the laser wavelength.

## 3. Laser Characterization and Optimization

In order to evaluate the laser performance of our structure, the 7-QW  $\frac{1}{2}$ -VCSEL was placed in a three-mirror cavity, and optically pumped with a laser diode module from Brightpower emitting up to 5 W at  $\lambda_p = 690 \text{ nm}$  on a 100  $\mu\text{m}$ -diameter-core fibre. The laser cavity consists of a  $R_C = 100\text{-mm}$  concave mirror with a high reflectivity ( $R > 99.97\%$ ) at  $\lambda_l = 852 \text{ nm}$ , and a plane output coupler (Figure 3). The semiconductor structure was simply fixed on a copper heatsink which temperature  $T_{sub}$  was controlled by a Peltier cooler.

We optimized the pump beam radius and the transmission of the output coupler to obtain the highest output power [20]. With a 40- $\mu\text{m}$  pump spot radius on the semiconductor structure we achieved a maximum output power of 330 mW for a pump power of 1.1 W and a  $T = 1.1\%$ -output coupler, at a substrate temperature  $T_{sub} = 0^\circ\text{C}$  (Figure 4). The slope efficiency next reached 35 %, and the overall optical-to-optical efficiency was 30% with regard to the incident pump power (35% with absorbed pump power). The laser threshold was as low as 158 mW, corresponding to a pump intensity of  $3 \text{ kW/cm}^2$  in good agreement with the predictions from Figure 1. The laser line was 2-nm broad; the central wavelength shifted from 848 nm at the laser threshold to 855 nm at the maximum output power because of the pump-induced heating of the QWs.

The laser output power was limited by a strong thermal roll-over at 1.1-W incident pump power, induced by the high thermal resistance of the active device. Actually the 350- $\mu\text{m}$  thick GaAs substrate, which has not been removed in this work, contributes to more than 75% of the total heating of the  $\frac{1}{2}$ -VCSEL, with a thermal resistance  $R_{th} = dT_{QW}/dP_{inc}$  ( $T_{QW}$  : QWs temperature,  $P_{inc}$  : incident power) evaluated to  $\sim 145 \text{ K/W}$  out of 190 K/W for the whole structure. Nevertheless the maximum output power, one of the highest ever reported without any thermal management in that spectral range, demonstrates the well-thought design of the active structure, as well as its growth quality.

## 4. Single-frequency operation in a compact prototype

### 4.1 Description

With the aim to develop a low-power single-frequency source dedicated to the detection of Caesium atoms, a compact monolithic external cavity with improved thermal and mechanical stability has been designed. We chose a single-transverse-mode laser diode as the pump source in order to limit intensity noise transfer from the pump to the laser emission [21]. The pump was thus a commercial Mitsubishi red laser diode delivering up to 150 mW at 658 nm for an operating current of 245 mA. The pump beam was focused on a 20  $\mu\text{m}$  radius spot with a pair of aspheric lenses ( $f = 4.5 \text{ mm}$  /  $f = 12.7 \text{ mm}$ ), at the incidence angle of  $70^\circ$  relatively to the structure, which circularizes the elliptic shape of the incident pump beam on the semiconductor chip. The external cavity was formed by a 12 mm-concave mirror  $R = 99\%$  at 852 nm mounted on a piezo-electric transducer (PZT) (see Figure 5). The laser cavity length was carefully adjusted in order to optimize the overlap between the cavity mode and the pump one. The active structure is directly fixed on a thermoelectric (TE) cooler with thermal heatpaste, which allows to control its temperature with a precision better than  $10^{-3} \text{ K}$ . The temperature of the whole laser external cavity was separately stabilized with another TE element close to room temperature in the following. The pump system, the semiconductor chip and the external mirror have been integrated on the same mount. The overall setup fitted within a  $52 \times 52 \times 58 \text{ mm}^3$  cube, and was protected by acoustic isolating covers to improve both its thermal and acoustic isolation. Then the laser remains running for weeks without needs for re-alignment.

### 4.2 Laser operation without any intracavity frequency-selective element

In this compact prototype, the laser output power is limited by the available pump power to 17 mW (Figure 6) at a substrate temperature of  $10^\circ \text{C}$ . The threshold was reached for an incident pump power of 52 mW, and the slope efficiency was 17% (with regard to incident pump power) without any evidence of thermal roll-over up to the maximum 150-mW pump power. The emission was linearly polarized, and the beam was diffraction-limited with a quality factor  $M^2 < 1.1$ . The emitted wavelength shifted from 850.5 nm at threshold to 852.2 nm at maximum pump power.

Without any frequency-selective intracavity element, we observed a stable single-frequency operation within a large range of operating conditions of the substrate temperature and pump current, with a side-mode suppression ratio higher than 30 dB (measurement-limited). This was checked with a high finesse ( $F=130$ ) scanning Fabry Perot (Figure 6) with a free-spectral range (FSR) of 37.5 GHz larger than the FSR of the laser cavity. This is attributed to the nearly-ideal gain homogeneity of VECSELs sources which has been extensively studied in [14]. Actually the characteristic time needed for the laser spectrum to collapse to a single-mode is about 1 ms in our experimental conditions, faster than acoustic and thermal fluctuations in our laser set-up.

Concerning the wavelength tunability, the laser line shifts towards longer wavelengths, as the QWs gain does, either with the substrate temperature or the incident pump power. A broad tunability over 6 nm is thus obtained from 850 nm to 856 nm by changing the substrate temperature from  $7^\circ\text{C}$  to  $20^\circ\text{C}$ , with a rate of 0.24 nm/K which is typical for these AlGaAs-based materials. Furthermore the laser wavelength moves with the incident pump power at 17 pm/mW (with regard to the incident pump power).

### 4.3 Operation with an intracavity Fabry-Perot etalon

To force the laser wavelength independently of the operating conditions, we chose to insert a 26- $\mu\text{m}$  thick uncoated silica etalon inside the cavity. The laser wavelength is then only set by the etalon orientation over 9 nm, and does not change with either the temperature (over  $\Delta T = 30^\circ\text{C}$ ) or the available pump power. In the meantime the output power and the efficiency decreased respectively to 8 mW at the maximum available pump power and 12% with respect to the incident pump power; the threshold increased to 85 mW due to the extra losses introduced by the etalon. By tuning the external-cavity length with the piezoelectric transducer, we achieved a continuous tunability over 14 GHz (0.03 nm) without any mode hop. It is worth noticing that this large continuous tunability of the laser frequency, owing to our short-length cavity, is favourable in atomic physics experiments; actually it makes it possible to scan continuously the optical transitions of interest, distant from 9.192 GHz, corresponding to the hyperfine levels ( $6^2\text{S}_{1/2}$ ,  $F = 3$ ) and ( $6^2\text{S}_{1/2}$ ,  $F = 4$ ) of the  $^{133}\text{Cs}$ -atom ground state. A Doppler-free saturated-absorption spectrum of the ( $6^2\text{S}_{1/2}$ ,  $F = 4$ )  $\rightarrow$  ( $6^2\text{P}_{3/2}$ ,  $F'$ ) transitions obtained in a Cs gas cell is shown in Figure 7. The  $\sim 5\text{-MHz}$  wide hyperfine lines are clearly resolved.

### 4.4 Evaluation of the spectral properties

With the etalon inside the cavity, the laser frequency has been locked at the side of a Doppler-free transition of the D<sub>2</sub> line, through a low-frequency ( $f < 2 \text{ kHz}$ ) 2-integration-stage servo loop on the piezoelectric transducer. The root-mean-square (RMS) frequency error signal, which is an evaluation of the global frequency fluctuations of the OP-VECSEL relatively to the atomic reference, is assessed at 300 kHz over 10 s and above (inset in Figure 7). We have checked that the intensity noise (RIN) remains negligible and do not contribute significantly to these measurements. The power spectral density of the frequency noise, measured from the error signal with a Fast Fourier Transform analyser, reveals that the main contributions to the laser frequency noise are below

100 kHz, and are attributed to residual electronic and acoustic instabilities of the set-up (Figure 8). A strong correction of the frequency fluctuations is obtained below 1 kHz. In the high frequency range, the white noise floor of the frequency noise spectrum reached  $\sim 13 \text{ Hz}^2/\text{Hz}$ , which would correspond to a Schawlow-Townes fundamental linewidth of 40 Hz [22]; this value is within the order of magnitude of the theoretical limit for a 10 mm-long external-cavity semiconductor laser.

The laser linewidth of our source has been further validated through the beat note measurement between our OP-VECSEL and an extended-cavity diode laser (ECDL) similar to the one described in [4], which linewidth has been previously evaluated to 130 kHz at -3 dB. In order to suppress low-frequency drifts of the laser frequencies, the OP-VECSEL and the ECDL were locked to distinct sub-Doppler Cs lines. The beat note signal around  $F_0 = 135 \text{ MHz}$  was detected by a fast InGaAs photodiode, then amplified and measured with a radio-frequency spectrum analyzer. The relevant time scale for the evaluation of the laser spectrum is the typical light/atoms interaction duration in atomic physics experiments, in the 10-ms range for atoms detection in Cs clocks. Thus the full width at half maximum of the beat note measured over 10 ms is 500 kHz, which is mainly attributed to the OP-VECSEL (see Figure 9). Actually assuming Gaussian shapes for both laser lines, the VECSEL linewidth is  $\sim 480 \text{ kHz}$ . The FWHM of the Lorentzian fit of the spectrum wings ( $|\nu - \nu_0| > 1 \text{ MHz}$ ) is 70 kHz – 55 kHz imputed to the VECSEL line, which is still larger than our previous evaluation of the ultimate linewidth from the white-noise magnitude; this is regarded as a consequence of the low-frequency extra acoustic, thermal and electrical noise peaks observed in the error signal spectrum (Figure 7) which are unavoidable under normal laboratory environment. Indubitably the laser linewidth could still be reduced with a better control of our environmental conditions and an enlarged servo bandwidth.

## 5. Conclusion

By giving extra care to the conception and the fabrication of the semiconductor component, we have demonstrated a diode-pumped VECSEL emitting at 852 nm with a low threshold intensity ( $I_{\text{th}} = 3 \text{ kW/cm}^2$ ). We have obtained a 330-mW laser emission around 852 nm from a structure on a GaAs substrate, without any complex additional thermal management nor post-processing of the wafer.

From a low-power compact prototype we have obtained a pump-limited output power of 17 mW under single-frequency operation on the Caesium D<sub>2</sub> transition. The spectral tunability of the source around the desired optical frequency was at least 14 GHz without mode-hopping. Moreover the laser has been locked to an absolute atomic reference, and complete frequency noise measurements have been performed. The residual frequency fluctuations of the laser line as compared to the atomic transition were about 300 kHz RMS over 10 s. Last but not least an independent evaluation of the laser linewidth through a beat-note experiment has established that the FWHM laser linewidth was below 500 kHz over 10 ms. We believe that this work results in an actual characterization of the frequency noise of a single-frequency VECSEL under single-mode diode pumping.

Finally the potentialities of a diode-pumped VECSEL as an alternative in the optical source architecture of Caesium atomic clocks have been investigated. Our laser performance are already adequate for optical detection of atoms in these setups. The further increase of the output power will require a reduction of the thermal resistance of the semiconductor chip in order to withstand high-power pumping. We could utilize well-established solutions as long as they remain compatible with the tunability of the single-frequency emission attempted here, such as substrate removing, bonding to a high-conductivity substrate or intracavity wedged heatspreader technique [23].

## Acknowledgements

This work has been partly supported by the Délégation Générale à l'Armement (Poseida N°0534004) and the Agence Nationale de la Recherche (ANR-07-BLAN-0320-03). B. Cocquelin acknowledges the CNRS and CNES for the funding of his PhD.

# List of references

1. A. Clairon, P. Laurent, G. Santarelli, S. Ghezali, S. N. Lea, M. Bahoura, IEEE Trans. Instr. Meas. **4**, 128 (1995)
2. P. Laurent, M. Abgrall, C. Jentsch, P. Lemonde, G. Santarelli, A. Clairon, I. Maksimovic, S. Bize, C. Salomon, D. Blonde, JF Vega, O. Grosjean, F. Picard, M. Saccoccio, M. Chaubet, N. Ladiette, L. Guillet, I. Zenone, C. Delaroche, C. Sirmain, App. Phys. B **84**, 683 (2006)
3. B. Canuel, F. Leduc, D. Holleville, A. Gauguier, J. Fils, A. Virdis, A. Clairon, N. Dimarcq, Ch. J. Borde, A. Landragin, Phys. Rev. Lett. **97**, 010402 (2006)
4. P. Cheinet, F.P. Dos Santos, T. Petelski, J. Le Gouët, J. Kim, K.T. Therkildsen, A. Clairon, A. Landragin, App. Phys. B **84**, 643 (2006)
5. M. Fleming and A. Mooradian, IEEE J. Quant. Elec. **17**, 44 (1981)
6. S. Stry, S. Thelen, J. Sacher, D. Halmer, P. Hering, M. Mürtz, Appl. Phys. B **85**, 365 (2006)
7. R. Nyman, G. Varoquaux, B. Villier, D. Sacchet, F. Moron, Y. Le Coq, A. Aspect, P. Bouyer, Rev. Scient. Instr. **77**, 033105 (2006) <http://hal.archives-ouvertes.fr/hal-00014931/fr/>
8. D. Voigt, E.C. Schilder, R.J.C. Spreeuw, H.B. van Linden van den Heuvell, App. Phys. B **72**, 279 (2001)
9. A. Klehr, H. Wenzel, O. Brox, F. Bugge, G. Erbert, T-P. Nguyen and G. Tränkle, Proc. SPIE **6909**, 69091E, (2008)
10. M. Gilowski, Ch. Schubert, M. Zaiser, W. Herr, T. Wübbena, T. Wendrich, T. Müller, E.M. Rasel, W. Ertmer, Opt. Comm. **280**, 443 (2007)
11. M. Kuznetsov, F. Hakimi, R. Sprague, A. Mooradian, IEEE J. Selec. Topics in Quantum Electron. **5**, 561 (1999).
12. A. C. Tropper, H. D. Foreman, A. Garnache, K. G. Wilcox, and S. H. Hoogland, J. Phys. D **39**, R74 (2004).
13. J. Chilla, S. Butterworth, A. Zeitschel, J. Charles, A. Caprara, M. Reed, L. Spinelli, Proc. SPIE **5332**, 143 (2004)
14. A. Garnache, A. Ouvrard, and D. Romanini, Opt. Express **15**, 9403(2007) <http://www.opticsinfobase.org/abstract.cfm?URI=oe-15-15-9403>
15. M. Jacquemet, M. Domenech, G. Lucas-Leclin, P. Georges, J. Dion, M. Strassner, I. Sagnes, A. Garnache, App. Phys. B. **86**, 503(2007)
16. A. Ouvrard, A. Garnache, L. Cerutti, F. Genty, D. Romanini, IEEE Photon. Techn. Lett. **17**, 2020 (2005)
17. M. Holm, D. Burns, A. Ferguson, M. Dawson, IEEE Photon. Technol. Lett. **11**, 1551 (1999)
18. R. H. Abram, K. S. Gardner, E. Riis and A. I. Ferguson, Opt. Exp. **12**, 5434 (2004) <http://www.opticsinfobase.org/abstract.cfm?URI=oe-12-22-5434>
19. L. Coldren and S. Corzine, *Diode Lasers and Photonic Integrated Circuits* (John Wiley & Sons, 1995)
20. B. Cocquelin, G. Lucas-Leclin, P. Georges, I. Sagnes, A. Garnache, Proc. SPIE **6871**, 687112 (2008)
21. G. Baili, F. Bretenaker, M. Alouini, L. Morvan, D. Dolfi, I. Sagnes J. Light. Techn. **26**, 952 (2008)
22. K. Petermann, *Laser Diode Modulation and Noise* (Kluwer Academic Publishers, 1988)
23. A. J. Maclean, A. J. Kemp, S. Calvez, J.-Y. Kim, Taek Kim, M. D. Dawson and D. Burns, IEEE J. Quant. Elec. **44**, 216 (2008)

### List of figure captions

Figure 1: Threshold intensity vs. number of quantum wells in the structure for different intracavity losses  $L$  : 0.5%, 1% and 2% at  $T_{QW}=10^{\circ}\text{C}$  and  $40^{\circ}\text{C}$ , following Equation (1).

Figure 2 : Design of the semiconductor structure.

Figure 3: Experimental setup for OP-VECSEL optimization

Figure 4: Laser output power and laser wavelength vs. incident pump power at the substrate temperature  $T_{\text{sub}} = 0^{\circ}\text{C}$ .

Figure 5: Photograph of the low-power single-frequency prototype.

Figure 6: Laser output power vs. incident pump power in single-frequency operation at  $7^{\circ}\text{C}$ ; inset: transmission of the scanning 37.5 GHz-FSR Fabry-Perot demonstrating single-frequency operation.

Figure 7 : Doppler-free Cs absorption spectrum in a vapor cell, from the ( $6^2\text{S}_{1/2}$ ,  $F = 4$ ) hyperfine ground state; inset : error signal measured at the side of the atomic line.

Figure 8: Spectral density of the error signal with/without optimized servo gain

Figure 9: Beat note measurement between the VECSEL and a known ECLD. The resolution bandwidth is 10 kHz, the sweep time is 20 ms; the signal has been averaged 10 times.

Figure 1

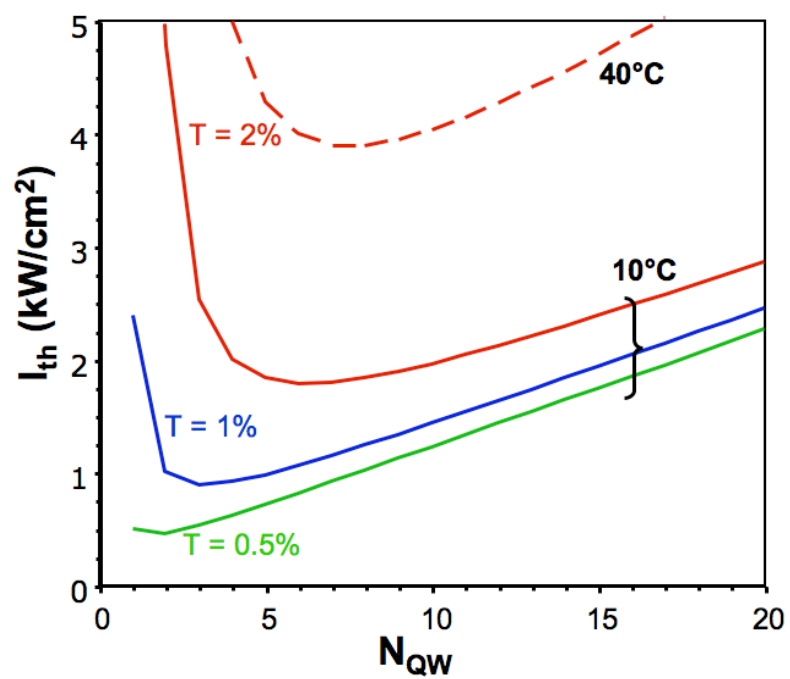




Figure 2

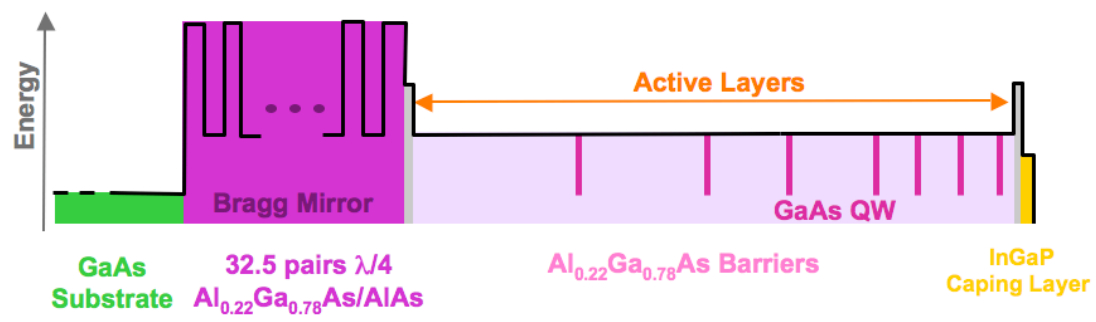


Figure 3

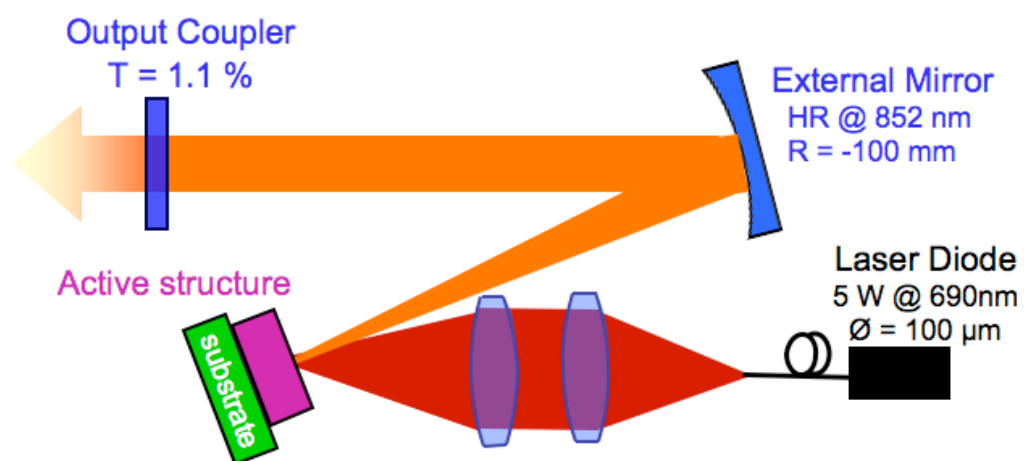


Figure 4

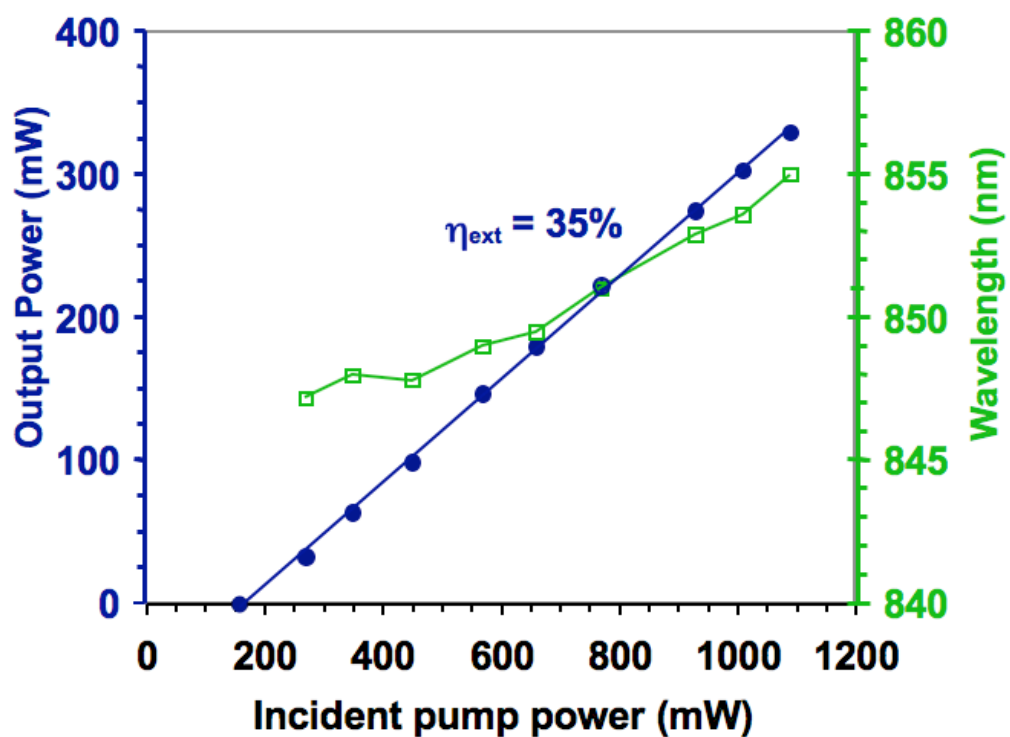


Figure 5

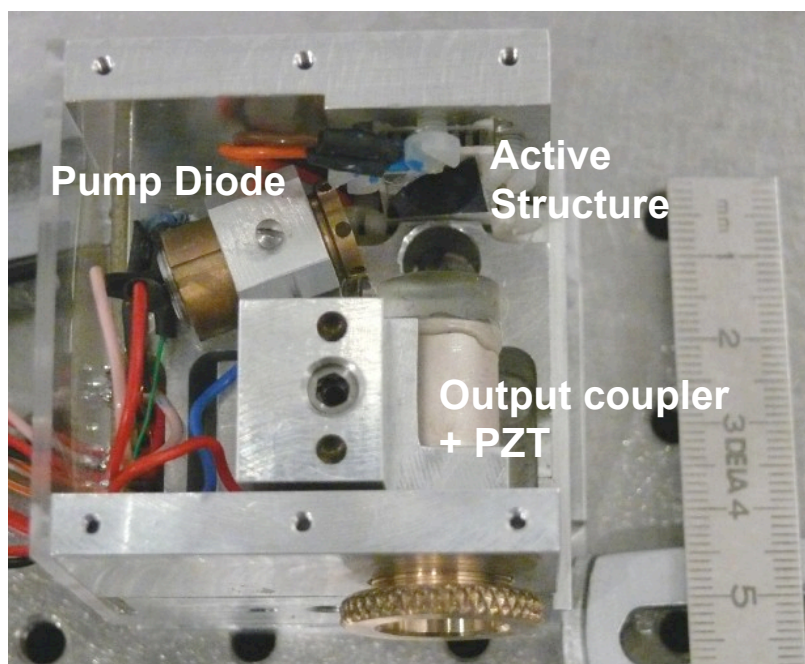


Figure 6

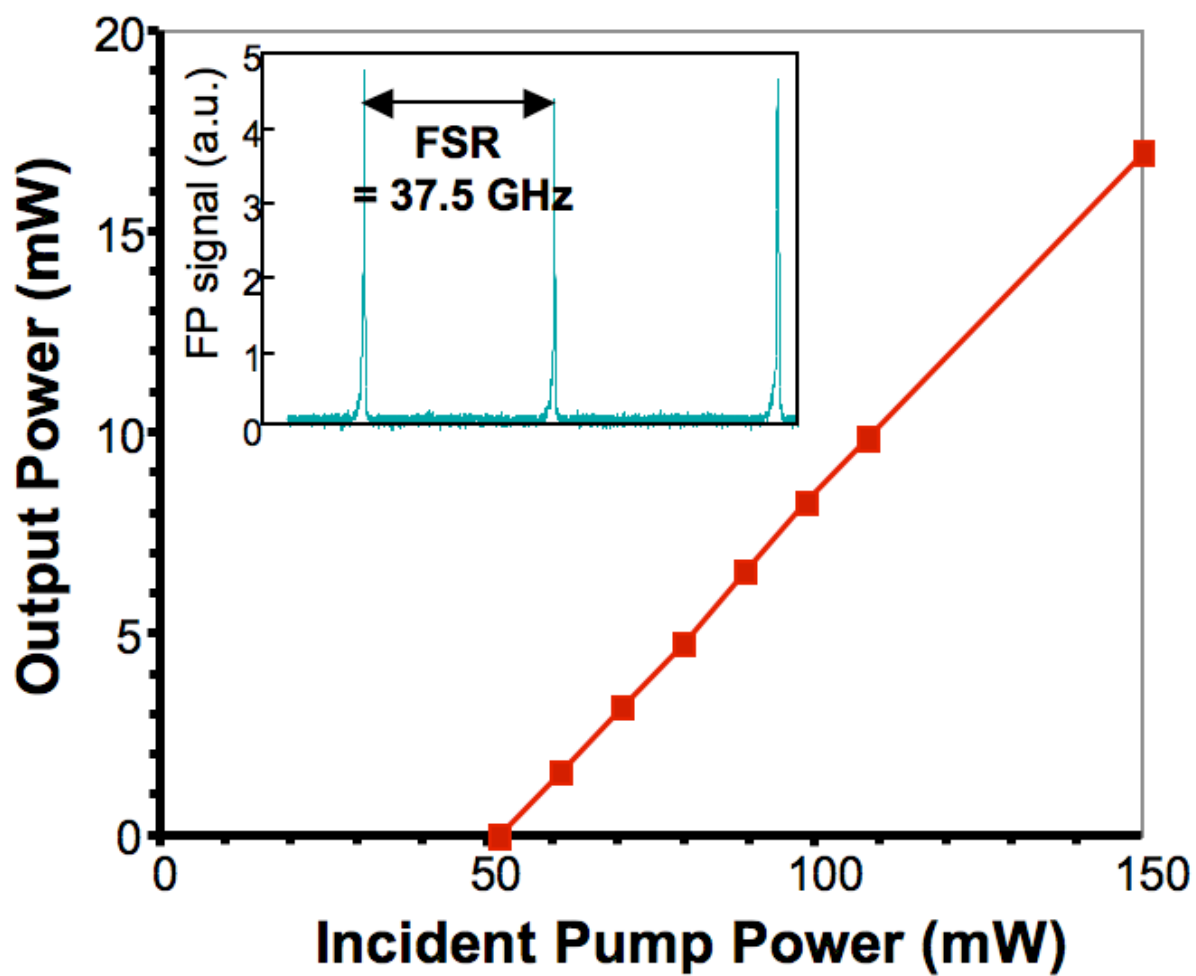


Figure 7

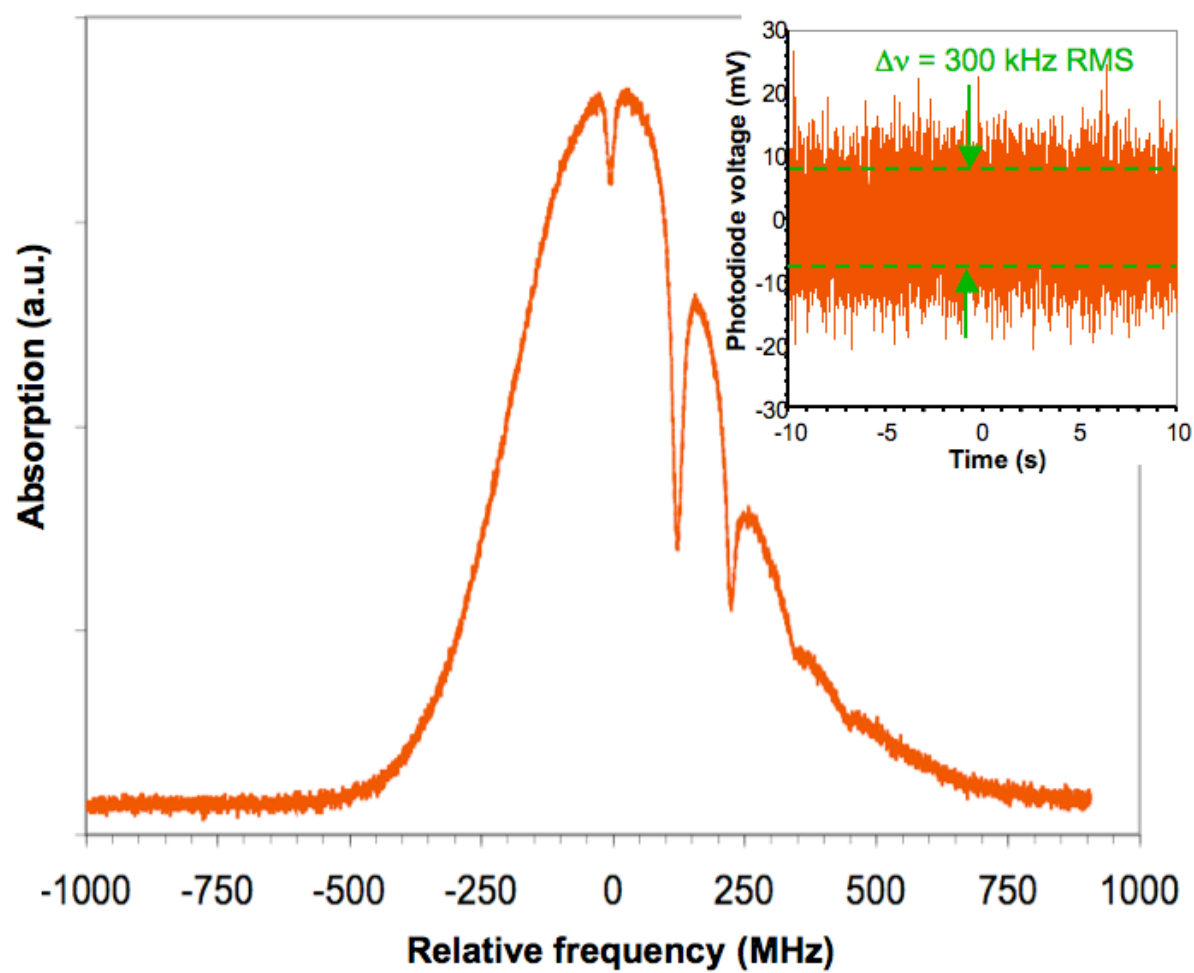


Figure 8

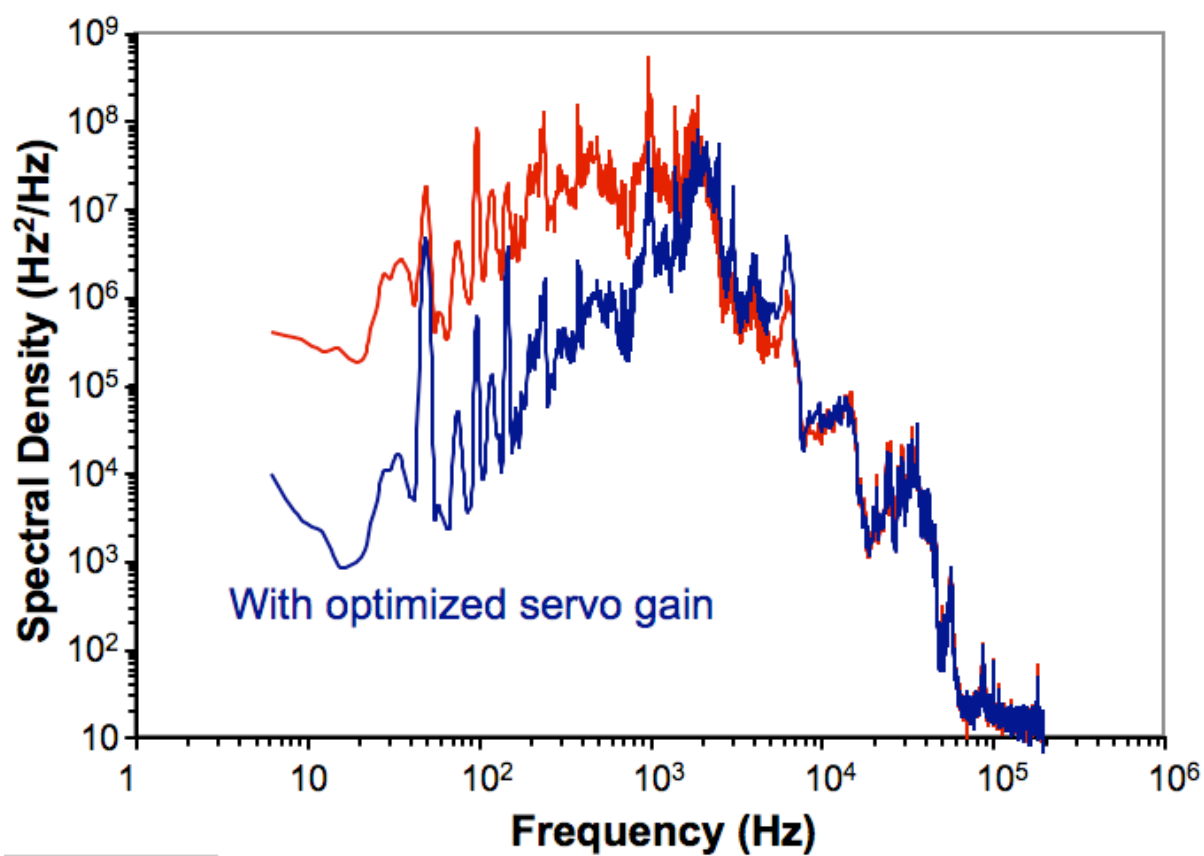


Figure 9

